Tribology International 120 (2018) 455–464

Contents lists available at ScienceDirect

Tribology International

journal homepage: www.elsevier.com/locate/triboint

A novel approach to minimize dry sliding friction and wear behavior of epoxy by infusing fullerene C_{70} and multiwalled carbon nanotubes

R.K. Upadhyay, A. Kumar *

Department of Mechanical Engineering, Indian Institute of Technology Kanpur, Kanpur, 208016, India

ARTICLE INFO

Keywords:
Fullerene
Multiwalled carbon nanotubes
Friction
Wear

ABSTRACT

This study investigates an in-depth analysis of chemical, physical, thermal and tribological behavior of infused epoxy matrix for applications lowering of dry friction is targeted. Epoxy substrates were prepared by infusing Fullerene C_{70} and Multiwalled Carbon Nanotubes in the weight concentration of 1, 3 and 5 wt%. Thermal analysis showed high glass transition temperature of carbon fillers compared to the pure epoxy substrate. These substrates have shown better surface wettability and increased surface energy at higher filler concentration. Friction coefficient and wear rate of tested filler epoxies ranges between 0.07 and 0.29 and 10^{-3}-10^{-2} mm^3/N-m. Increase in filler concentration up to 5 wt% showed significant improvement towards substrate tribological behavior.

1. Introduction

Over the years, the main goal of the manufactures is to develop machines to serve and fulfill the needs of human being. These machines are playing a pivotal role in day-to-day life ranging from basic machines to sophisticated machines simplifying the manufacturing processes to fulfill present and future needs. Nevertheless, many manufacturing uncertainties are associated with these machines, such as material selection, process parameters, overall economy, overall efficiency and lifetime service period with the operating and environmental conditions [1,2]. Selecting a particular factor amongst these and ignoring others can result in machine failure. Machine operating conditions, such as speed, load, duration, and counterpart material affect the performance in terms of material loss from the contacting surfaces of the machineries. Further, the environmental factors, such as temperature and humidity critically affect the materials behavior in terms of friction and wear. High humidity causes surrounding gases to convert into vapour phase and thereby reduces the friction coefficient [3]. On the other hand, increase in temperature results in high friction coefficient and wear rate. Keeping these factors in mind, the manufacturing unit requires extensive attention towards designing of individual machine components. As these components are operating under influencing contact condition, machine design requires better understanding of the tribological behavior of materials. Tribological study includes two bodies under sliding/rolling contact, where asperity contact dominates the surface friction and wear behavior under dry contact condition with or without particle impingement [4,5]. In order to minimize surface friction and wear, solid and liquid lubricants are deployed in between the contacting zone to eliminate the direct asperity contact. Some of the surface tends to deform or fail as soon as the load is applied to it, which requires preventive actions (material selection, operating condition and environmental factors) to overcome surface deficiency. Failure modes, such as fatigue, fretting fatigue, corrosion, erosion, cavitation, abrasion and adhesive failure [6–8] require proper attention towards better tribological design. In early time, scientist were involved in controlling the tribological losses through various techniques, such as surface modification techniques via various thin film deposition processes, lubrication by solid particles, lubrication by liquid intermittent contact between two moving parts, etc [9–11]. These techniques are still utilized, however, in recent times, search of self propelled materials with unique features triggered the need of extensive research in the field of tribology. In this regard, carbon materials [5,12–14] are gaining tremendous attention for their unique tribological properties obtained via synthesis mode.

In view of recent trends in nano material synthesis, requirements of novel light weight tribological materials [15] triggered the need of nano-micro scale fabrication. To fulfill the tribological requirement, incorporation of nano-micro scale materials as infusion into the base material can provide the suitable tribological properties [4]. Polymers [16] are one of the most reliable and cost effective materials for creating components with complex shape and varying size by using the molding process. Various techniques were developed to synthesize graphene based polymers [17] in emulsions, suspensions and dispersion medium.

* Corresponding author.
E-mail address: arvindkr@iitk.ac.in (A. Kumar).

https://doi.org/10.1016/j.triboint.2018.01.028
Received 16 November 2017; Received in revised form 27 December 2017; Accepted 11 January 2018
Available online 13 January 2018
0301-679X/© 2018 Elsevier Ltd. All rights reserved.

The emulsion polymerization is proved to be better compared to other techniques as it allows uninterrupted control of heat and viscosity without affecting the rate of polymerization. Further, addition of nano fillers [18–20] into these polymers provided enhanced properties, such as high tensile strength, hardness, yield strength, thermal and chemical resistance with low friction coefficient and high wear resistance. These nano fillers can be chosen on the basis of their physical and chemical structure, and mechanical properties. For instance, polytetrafluoroethylene (PTFE), carbon fibers, alumina, glass fibers, mica flakes, nanoclays, talc, zinc and boron are some of the filler materials [21–24].

Epoxy resin has been widely used as structural materials in aerospace, military, automobile, marine, space shuttle, cryogenics fuel tanks, biomedical system, and as non-conductive materials [25]. Although, epoxy has many applications in science and technology, its brittle behavior is a serious concern. It causes frequent and rapid crack propagation, which can lead to sudden breakage of the component. Addition of either rubber or polymer plastic, and inorganic [26] based filler infusions (like ceramic infusions) increases the fracture toughness which resists crack formation. Addition of graphene [27] as a filler material in polymer matrices improves mechanical, thermal and electrical properties with large surface area than any other infusions. Moreover, by adding graphene, other desired properties, such as chemical, physical and optical can be preciously tailored according to the functional requirement. In a similar way, addition of nano sized filler materials, such as fluoroepoxy oligomer diglycidyl of trifluoromethyl aniline (DGTFA), carbon fillers, graphite lubricants, polyetheretherketone (PEEK), nano silicon dioxide (SiO_2), titanium dioxide (TiO_2) and copper oxide (CuO) nanoparticles successfully reduced the friction coefficient and wear rate [28–30]. The effect of graphene oxide content on friction behavior is studied by Fu et al. [31] by varying the oxide content from very low weight fraction of 0.05 to 0.5 wt%. The measurement showed substantial reduction in friction coefficient. The effectiveness of nano graphene oxide resulting in higher available area is also projected. A significant wear resistance values were achieved when particles of alumina (Al_2O_3), silicon nitride (Si_3N_4), silicon dioxide (SiO_2) and graphene nano sheets were added to the epoxy solution [31]. Ye et al. [32] have tested the nano silica content for its tribological behavior and found that friction coefficient and wear rate have been reduced significantly as nano silica content changes from 10 wt% to 20 wt%. Ma et al. [33] experimentally studied the effect of nano-rubber in a matrix and showed that addition of nano rubber up to 5 wt% reduces specific wear rate and friction coefficient. However, more addition leads to formation of nano-rubber agglomerate causing substantial reduction in the hardness of nanocomposites which eventually leads to drastic increase in specific wear rate. The friction coefficient of multiwalled carbon nanotubes and fullerene has been studied experimentally under silicon/steel contact mode and values are found to be high ranging from 0.4 to 1.0 [34–37]. The high friction coefficient is due to molecular bonding between the substrate and counterpart steel ball. The friction is also higher because of adherence of surface grit particles at either side of the contacting bodies.

To the best of authors' knowledge there are some literature that quantified the tribological properties of steel/multiwalled carbon nanotubes and silicon/fullerene, however, till date any comprehensive work demonstrating tribological effectiveness of epoxy/fullerene C_{70} and epoxy/multiwalled carbon nanotubes are still lacking. Although infusion of filler materials in epoxies enhances mechanical, tribological and adhesion properties substantially, it has some limitations, such as inhomogeneous dispersion of nanoparticles, sedimentation and accumulation of particles at the base, chances of inducing brittleness into the substrate for inadequate amount of nanoparticles, high friction and wear rate under severe load condition, etc. Thus, in continuation to the previous developed methodology [34,36,37] which lacks in better material selection and tribological behavior, this work aims to modify surface friction and wear resistance by selecting new novel material composition based on their surface functionalization. In this regard, carbon materials, i.e., fullerene C_{70} and multiwalled carbon nanotubes have been selected to test the tribological properties of epoxy based composites. The selected carbon material as infused filler has been added to the epoxy solution in 1 wt%, 3 wt% and 5 wt%. In-depth analysis of sliding pair friction and wear mechanism with materials chemical, physical, thermal, and tribological behavior has been performed.

2. Experiment

2.1. Materials

Fullerene and multiwall carbon nanotubes (MWCNT) were purchased from PlasmaChem GmbH having purity of >99% and >95%, respectively. Length of the multiwalled carbon nanotubes was in the range of 1–10 μm with 3–15 numbers of walls. Epoxy resins Araldite CY230 and hardener Aradur HY951 were purchased from Huntsman Corporation. Bearing steel SAE 52100 balls were used as sliding counterpart material and it has the chemical composition as, C: 0.98, Mn: 0.25, Si: 0.15, Cr: 1.3, S: 0.025 and P: 0.025 (wt.%).

2.2. Epoxy substrate preparation

Epoxy substrates were prepared by mixing 1 wt% fullerene into the epoxy resin thoroughly with the help of an ultrasonicator for 15-20 min at 80 °C. Further hardener in the ratio of 100:10 (Epoxy resin:hardener) is added to the epoxy solution and mixed thoroughly for another 15 min. Afterwards, prepared substrates (Ø 20 mm, 5 mm height) were cured at room temperature for 1 h and subsequently at 100 °C for another hour. Other epoxy substrates of fullerene (3 wt% and 5 wt%) and MWCNT (1 wt%, 3 wt% and 5 wt%) were prepared in a same way. These substrates were then subjected to physical, chemical and tribological testing. Multiwalled carbon nanotubes have issue of homogeneous dispersion and because of that they tend to accumulate at the base. Care was taken by stirring the mixture for more time than the usual in order to break the agglomerates.

2.3. Characterization and surface property measurement

Fourier Transform Infrared Spectroscopy (FTIR, Thermo Scientific Nicolet 8700) was used to analyze corresponding bond between the atoms at a particular wave-number. X-ray diffraction (XRD, Panalytical) analyses were carried out to identify the presence of different phases in the prepared substrates. Microstructure analysis of epoxy substrates was performed by Scanning Electron Microscopy (SEM- FEI Quanta 200) at 10 kV at a scale of 300 μm. Substrates of pure epoxy, epoxy fullerene and epoxy MWCNT are characterized by XPS (PHI 5000 Versa Prob II, FEI Inc.) for its chemical state and presence of bonding state. The influencing bonding state is generally carbon-carbon and carbon-oxygen at the utilized scan rate of 50 ms/step (0.05 eV).

Thermal analysis of cured epoxies has been performed by Themogravimetry analyzer (TGA, STA 8000 Perkin Elmer Ltd.) to identify the glass transition temperature. Goniometer Data Physics OCA (Optical Contact Angle) was used to measure water and paraffin oil (64 cSt) contact angle by using droplet of 0.2 μl. Total three measurements has been performed to estimate average contact angle value. Surface roughness and sliding wear track of the prepared epoxy substrates have been observed by 3D optical profilometry (Contour GTK, Bruker, USA) and optical microscopy (Nikon Eclipse Confocal Optical Microscope, LV100). The worn surfaces of steel balls were also observed under optical microscope. Specific wear rate of all epoxy substrates was calculated by the following formula.

$$W_{sp} = V/LD \quad (1)$$

where V is the wear volume, L is the normal load and D is the total sliding distance.

To estimate the wear volume, first width and depth profile of the wear

track have been added and then it was multiplied by the total wear track length. The hardness of epoxy substrate has been measured by Vickers hardness tester (Tinius Olsen-FH 10, Netherland) at normal load of 5 N. Total five indents were made and average value of these five measurements has been reported.

2.4. Ball on disk tribometer

The prepared epoxy substrates were tested by ball on disk tribometer for determining their coefficient of friction (COF) and wear rate values. In this test a steel ball of 4 mm diameter and hardness of 58 HRC is fixed in a cylindrical rod and slides against a rotating disk (see Fig. 1). The sliding velocity and the disk rotational speed were 0.28 m/s, 1000 RPM respectively. For friction measurement, a strain gauge is provided adjacent to the ball holder. As the epoxy substrate is pressed by the action of applied load, some amount of deflection is fed towards the strain measurement system through strain gauge to calculate the value of the friction force. Then strain measurement system converts the analog signal obtained from the strain gauge to the digital signal with the help of data acquisition system. This digital output voltage signal is then recorded by the Labview™ software which is then multiplied by the calibration factor (0.75 N/mV) of the load cell to calculate coefficient of friction.

3. Results and discussion

In order to investigate structural phases of the prepared epoxy based fullerene C_{70} and multiwalled carbon nanotubes samples an XRD analysis was performed (see Fig. 2). All the presented peaks are for 1 wt% epoxy filler substitutes. After addition of fillers into the epoxy matrix, the structural peak changes compared to the pure epoxy substrate due to internal chemistry between the epoxy and other filler materials. It can be seen that pristine fullerene has a broad peak at (110), (103) and (112) planes. On the other hand pristine MWCNT yields (002) plane at 26.5° which is quite similar to the graphite powder [38]. However, addition of these carbon materials into the epoxy yields some shift in the behavior due to the change in crystal structure. As seen, pure epoxy has a peak at an angle of 20.2° but the peak for epoxy fullerene is at an increased angle of 20.77°. For MWCNT epoxy samples, the peak occurs at a decreased angle of 19.88°. It clearly shows that addition of filler particles into the epoxy influences the interfacial interaction between the molecules by having a close molecule packaging which provides valued microstructure composition. The close molecule packaging at nearby surface provides dense microstructure and results in high hardness of the prepared substrates. The change in angle is due to the change in chemical composition, temperature and resulting strains for MWCNT epoxy nanocomposites. The planer stress shifts towards lower angle for the tensile stresses and towards higher angle for the compressive stresses due to shift in *d*-spacing [39]. From tribology point of view, any compressive stress developed in the sample will be able to hold the maximum load on the substrate surface without any surface flaw.

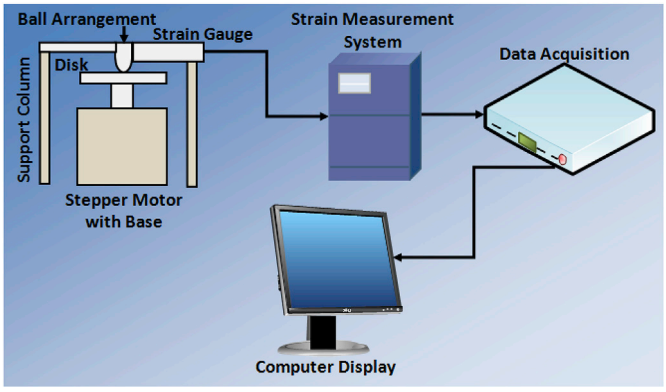


Fig. 1. Schematic diagram of ball on disk measurement.

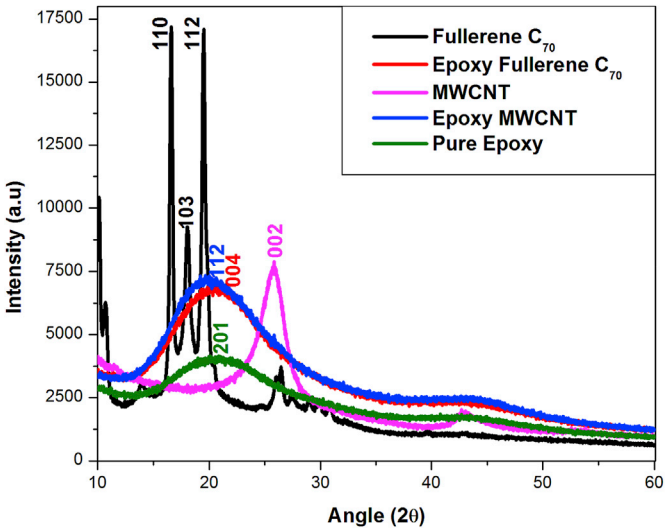


Fig. 2. XRD pattern of fullerene C_{70}, multiwalled carbon nanotubes, epoxy fullerene, epoxy MWCNT and pure epoxy. For all filler additions, the pattern of epoxy samples is similar but a small shift in their behavior is observed. This is caused due to the preparation and change in crystal structure.

The FTIR spectra of fullerene C_{70} and MWCNT as well as pure epoxy, epoxy fullerene C_{70} and epoxy MWCNT (1 wt%) are shown in Fig. 3. The excited vibration state denotes molecular structure at the particular wave-number. A number of large peaks appear towards the lower wave-number range for fullerene C_{70} and epoxy fullerene C_{70} due to presence of different molecular structures. The major peaks around 641.60, 673.49, 794.75, 651.05, 704.99 and 737.46 cm^{-1} represent aromatic C-H bending. However, peaks between 500 cm^{-1} and 600 cm^{-1} show major proportion of halide functional group. While moving towards the higher wave-number range, for epoxy fullerene, presence of = C-H, C-O, C=C, C=O, -C≡C- and O-H bonding [40] appears at 964.52, 1320.04, 1414.03, 1725.62, 2170, 3440.38 cm^{-1}, respectively. Similarly, C-O, C=C and O-H stretching vibration is also observed for fullerene C_{70} at 1320.04, 1429.24 and 3424.87 cm^{-1}. For pure epoxy sample, low stretching vibration of C-O, C=O and C-H is generally observed at 1090.08, 1885.14, 2846.75 cm^{-1}, respectively. MWCNT powder showed some intense peaks after 3500 cm^{-1}, termed as N-H stretching (presence of amines in the hardener), while marginal peak around 3500 cm^{-1} represents O-H stretching [41]. When MWCNT is blended with epoxy, more intense stretching peaks around 2100, 1609.96 and 3872.17 cm^{-1} are observed for the presence of -C≡C-, C=O, O-H bonding. The major proportion of hydroxyl and carbonyl group makes the sample molecules or content to dissolve in water.

The thermogravimetry analysis of the prepared epoxy substrates, i.e., epoxy fullerene C_{70} and epoxy MWCNT, is depicted in Fig. 4. In Fig. 4a, the three zones of thermal analysis as indicated under the blue segment, are the result of glass transition temperature (T_g), crystallization temperature (T_c) and melting temperature (T_m). Particle infusion certainly changes the glass transition temperature of the prepared epoxy substrate with filler as compared to pure epoxy substrate. The measured values are 46.10 °C, 59.13 °C and 58.17 °C for pure epoxy, epoxy fullerene C_{70}, epoxy MWCNT, respectively. Sometimes, the glass transition temperature of the tested filler epoxy substrate reduces towards lower value due to the softening (high heat absorbance capacity) of fullerene C_{70} and hollow structure of MWCNT in the radial direction, respectively [42]. The formation of crystals at increasing temperature is observed at around 150 °C for all the tested samples. With further increase in temperature, for the both samples a drastic change in behavior at the point of degradation or melting is observed past 300 °C. The effect of temperature on weight loss is indicated in Fig. 4b. The loss in weight is significant as the

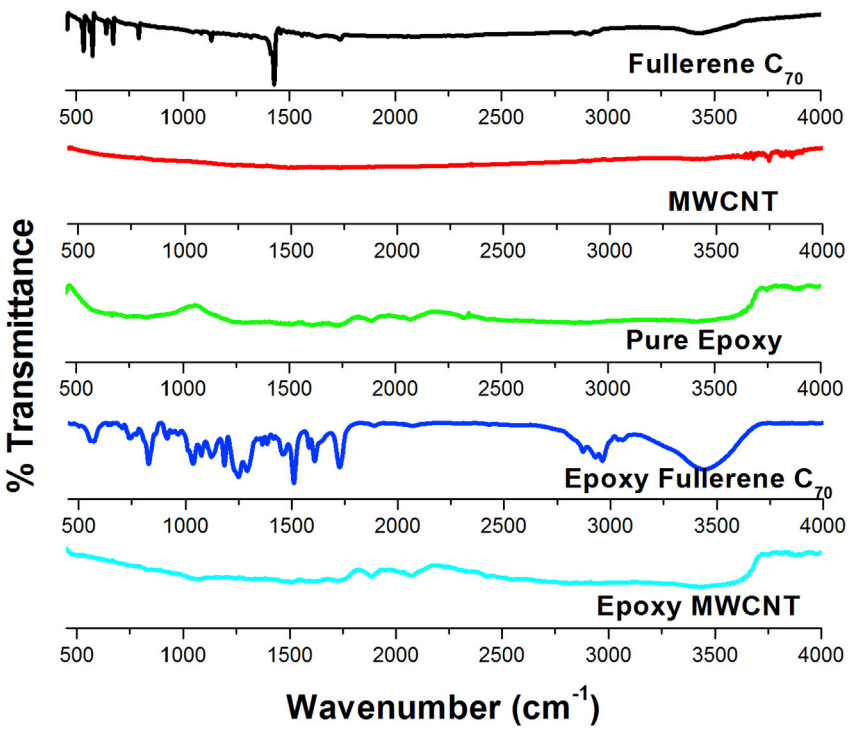


Fig. 3. FTIR spectra of fullerene C_{70}, MWCNT, pure epoxy, epoxy fullerene C_{70} and epoxy MWCNT. The broad peaks are obtained for fullerene C_{70} and epoxy fullerene C_{70} at low wave-number. However, some of the peaks were also observed at wave-number above 2800 cm^{-1} for epoxy fullerene C_{70}. Compared to fullerene C_{70} lower wave numbers have been observed for pristine MWCNT, epoxy MWCNT and pure epoxy.

temperature reaches above 150 °C which continues till 325 °C. Beyond this temperature the extreme adverse situation is reached and the material is degraded. Generally, loss in weight above 300 °C is attributed towards oxidation of carbon at high temperature. The glass transition temperature is an important aspect, and a higher value for this must be achieved by adopting an appropriate curing process and temperature limit. Low glass transition temperature causes the substrate to bend or break as soon as an external load is applied. On the other hand, high glass transition temperature avoids sudden breakage or distortion of the substrate. Addition of MWCNT and fullerene C_{70} in the epoxy matrix has shown higher glass transition temperature, those are very useful for high temperature operation (below 150 °C). The automotive engine normally works at a maximum temperature of 100 °C. The automotive engine components, such as fuel tank and valve operate in the range of 35–40 °C. For these applications the use of epoxy fullerene C_{70} and epoxy MWCNT as compared to traditional materials can offer significant weight reduction. Hence, these filler epoxies are the future trends for aiming a particular weight reduction design with increased hardness and improved tribological properties. The hardness and tribological properties of these filler epoxies are discussed in subsequent sections.

To study the chemical state, XPS analysis plot of cured epoxies (pure epoxy, epoxy fullerene C_{70} and epoxy MWCNT-1 wt.%) is shown in Fig. 5. Pure epoxy and other filler epoxies had their major peak of binding energy at about 283.5, 286 and 289 eV (see Fig. 5a.) which originates bonding state of C-C, C-O-C, O-C=O respectively. Fig. 5b show oxygen spectra binding energies at 531 and 533 eV, which represents C=O and C-O bonding respectively. The intense peak at 283.5 eV (C1s) corresponding to C-C bonds represents sp^3 hybridization [43]. The atomic concentration of the tested epoxies shows that pure epoxy had lower concentration of carbon than epoxy MWCNT and epoxy fullerene C_{70}. A little impurity in the form of oxygen originates while the curing process takes place from room temperature to 100 °C. These oxygen molecules have reacted with epoxy substrate surface and forms bonding with carbon atoms.

Contact angle and the corresponding surface energies of all the prepared epoxy substrates with varying dose of fullerene C_{70} and MWCNT filler concentration (1 wt%, 3 wt% and 5 wt%) have been shown in Fig. 6a and b. To estimate the surface wettability behavior, contact angle values of epoxy fullerene C_{70} and epoxy MWCNT was measured in the presence of water and paraffin oil. From the result of fullerene C_{70} a general observation can be made that increase in filler weight concentration decreases the contact angle values (see Fig. 6a). In the presence of water, the contact angle values of 1 wt%, 3 wt% and 5 wt% fullerene C_{70} are 67.3°, 63°, 61° respectively. However, pure epoxy has higher contact angle value of 96.65°. While comparing oil contact mode to water, it can be seen that the oil contact angle values are on much lower side. The contact angle as 10.9° is obtained with 5 wt% fullerene C_{70}. The epoxy matrix infused with MWCNT (Fig. 6b) has been also tested for its wetting nature under water and oil contact mode. Similar to fullerene C_{70}, MWCNT epoxy substrate with higher weight concentration had performed substantially better under both contact modes. The lowest achievable contact angle values are 56.9° and 11.7° in the presence of water and oil contact mode, respectively. The results indicate that addition of fullerene C_{70} and MWCNT into the epoxy significantly reduces the contact angle values. Higher filler concentration makes the prepared substrate surfaces hydrophilic in nature by improving its wettability. Although particle concentration increases the surface roughness, but depending upon the nature of peaks, fluid retained inside the valleys and thus lowers the contact angle. In the case where the roughness peak height is large, the fluid will provide rolling action instead of sliding, and in that case contact angle value will increase. Surface energy of the prepared epoxy substrate surfaces has been estimated by the equation of state theory [44,45], and it has been found that addition of fullerene C_{70} and MWCNT from low to high concentration continuously increases the surface energy. Thus surface energy had a positive impact on the hydrophilicity as all contact angle values are well below 90° with addition of high filler concentration into the epoxy matrix.

Contact angle or surface wettability are of great importance in friction and wear studies. The relation between wetting and tribological behavior totally depends on the surfaces characteristic of the testing material pair [46]. The variation in tribopair yields different results in presence of dry/lubricated contact. Friction coefficient and wear value of epoxy (with/without filler particles) surfaces against steel counterface in dry

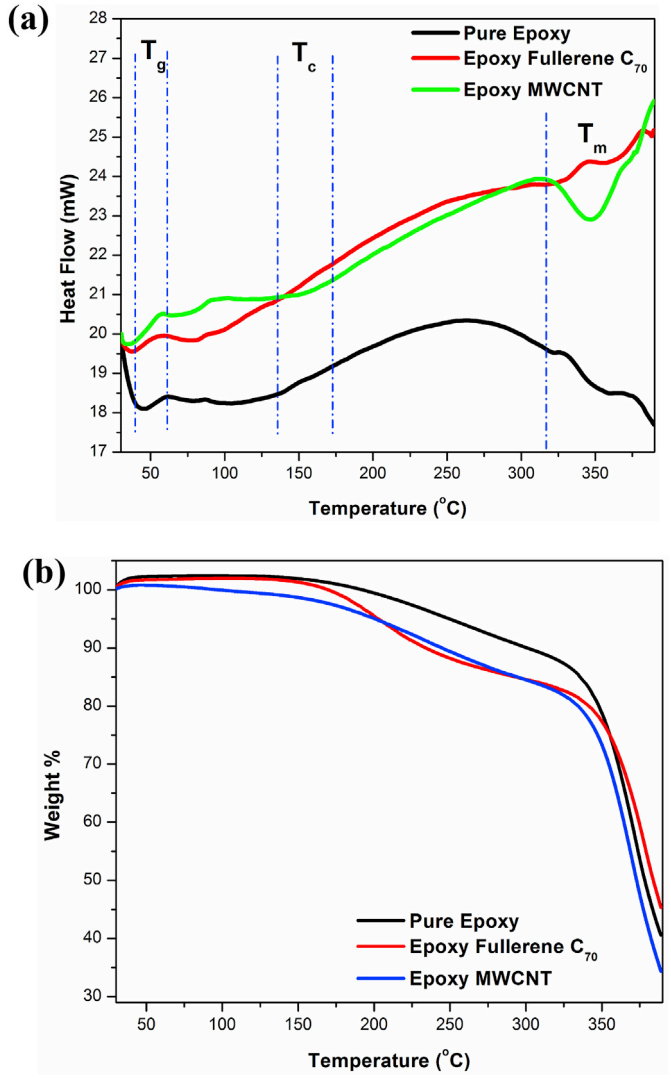


Fig. 4. (a) Thermal analysis of pure epoxy, epoxy fullerene C_{70} and epoxy MWCNT substrates from room temperature to 400 °C. Glass transition temperature (T_g) is the indication of initial change in phase of the prepared epoxy substrates while heating, crystallization temperature (T_c) is the indication of second change in phase of the material structure and melting temperature (T_m) is the indication of third phase change. (b) Weight loss of epoxies under temperature variation up to 400 °C. The two steep weight losses at 150 °C and 300 °C are the indication of release of the absorbed water molecules, and oxidation of carbon, respectively.

condition does not change considerably with increasing contact angle [47]. Pure epoxy substrate had higher contact angle (96.65°) and friction coefficient value (Fig. 7a-c) as compared to infused filler substrates. Surfaces with low and high water contact angle generally represent hydrophilic and hydrophobic characteristics, respectively [48]. The film thickness on the hydrophilic surfaces is thinner than on the hydrophobic surfaces, which provides increased adhesion on the outer surface due to strong bonding (ionic or covalent bonding - high energy surfaces), and thus increases the friction coefficient. However, as soon as the outer surface molecules are detached from the substrate, exposure with intrinsic bulk molecules having less surface energy occurs, which reduces the friction coefficient. On the other hand, hydrophobic surfaces having high film thickness reduces the friction coefficient due to presence of weak Van der Waals forces (low energy surfaces) [49].

The measured values of surface hardness and roughness parameter of the epoxy substrates have been reported in Table 1. As can be seen, increment in filler concentration increases surface hardness and roughness parameters. For both the substrates, high hardness was obtained for 5 wt% filler. Similarly, highest surface roughness was found for 5 wt% filler. The values of average roughness (R_a), root mean square roughness (R_q), maximum peak height (R_p) and maximum valley depth (R_v) are estimated by surface plot.

The average coefficient of friction (COF) values of tested pure epoxy and other epoxy substrates with varying concentrations of filler and loads are shown in Fig. 7a-c. Furthermore, SEM images of all the prepared substrates are illustrated in Fig. 8a-d and Fig. 9a-c. Pure epoxy substrate has relatively higher friction coefficient values at both load conditions due to severe accumulation of particles in the nearby of track area (see Figs. 7a and 8a). Addition of 1 wt% fullerene C_{70} has provided better friction coefficient behavior, see Fig. 7b. Under low load limit the COF value is at higher side (0.29) because of more particle detachment from the substrate surface and crack formation (see Fig. 8b). At high load condition, initial contact at the substrate surface causes rapid change in friction behavior due to sudden applied load and abrasive shearing. However, friction value was dropped once the steady state zone is achieved with occurrence of some smooth region. The formation of smooth region is a result of several attempt of sliding and buildup of transfer film formation. The lowest friction coefficient value has been found during sliding contact of 3 wt% fullerene C_{70} at different loads. The average COF value at 4N load is ~0.17. The lower value is attributed to lesser amount of adherent particles between the sliding contacts and smooth sliding between the ball and substrate material (see Fig. 8c). On the whole, it appears that substrate surface and counterpart material are not allowing the grit particles to accumulate in between, and hence lower friction coefficient value with minimum wear rate is observed, as shown in Fig. 10. Further, after continuous rubbing, the generated grit particles turned into a protective layer under the influence of load and sliding speed, which also contributes to lowering the friction coefficient. Further increment in weight concentration (5 wt%) at particular loads increases the friction coefficient values compared to 3 wt% filler. This rise is

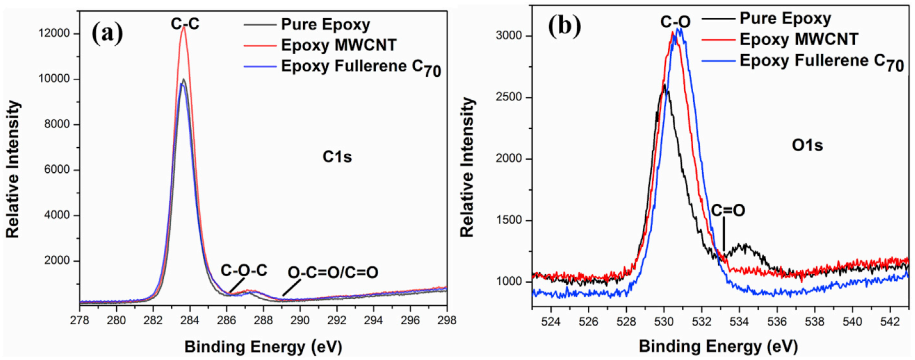


Fig. 5. XPS spectra of pure epoxy, epoxy MWCNT and epoxy fullerene C_{70}. (a) C1s spectra, (b) O1s spectra.

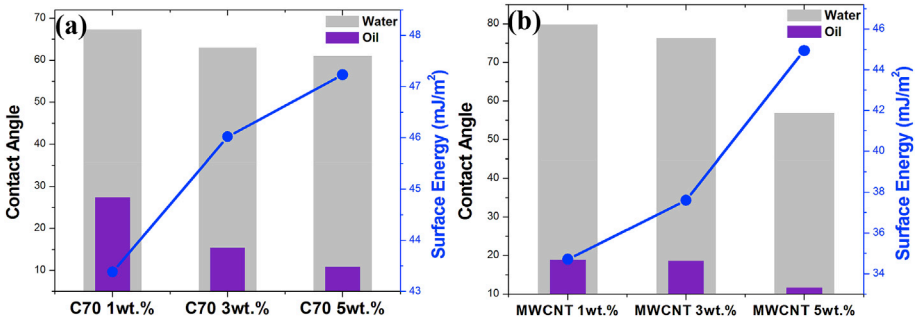


Fig. 6. Contact angle and surface energy of the prepared (a) fullerene C_{70} and (b) MWCNT epoxy substrates under water and oil mode.

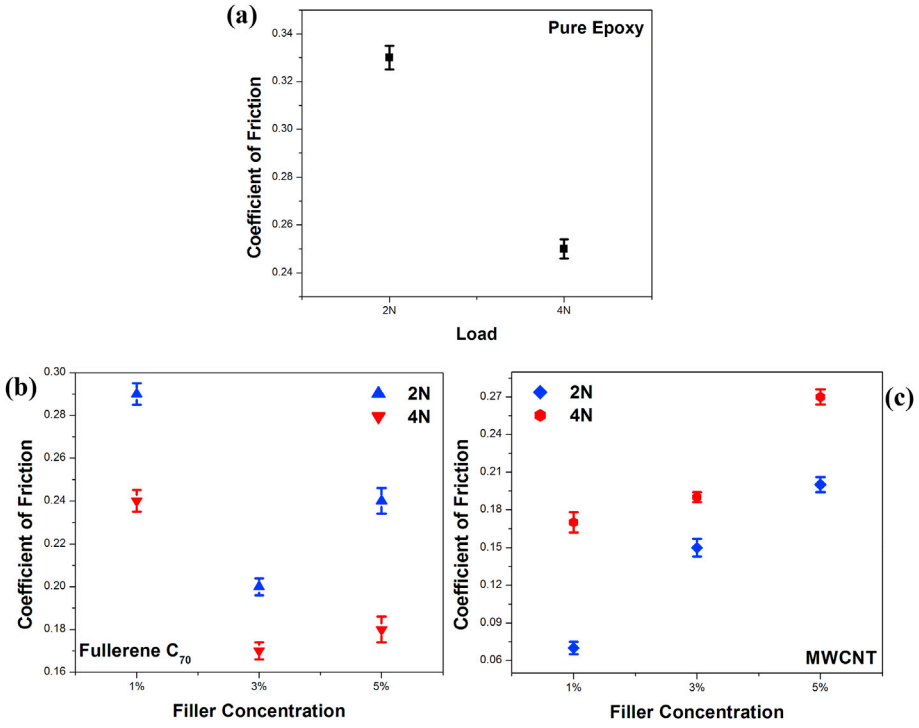


Fig. 7. Average friction coefficient value of (a) pure epoxy, (b) epoxy fullerene C_{70} and (c) epoxy MWCNT. Addition of filler decreases the friction coefficient values compared to pure epoxy. The three distinct phases of friction are: (i) Friction coefficient is higher due to sudden applied load, at this stage shearing of oxide film takes place which was built during open environment condition. (ii) Friction coefficient tries to lower down by providing protective film over the substrate surface but the film formation is underway and does not stabilized by this stage. (iii) After a while, protective film stabilizes which further lowers the friction coefficient. However, sometimes due to presence of surface flaw or any foreign particles, friction coefficient may increase.

Table 1
Measured hardness and surface roughness of prepared epoxy substrates.

	Hardness (HV)	Standard Deviation	Average Roughness (R_a)	Root Mean Square Roughness (R_q)	Maximum Peak Height (R_p)	Maximum Valley Depth (R_v)
C_{70} 1 wt%	9.57	0.17	0.465	0.584	3.126	−2.983
C_{70} 3 wt%	11.21	0.24	0.499	0.627	2.983	−3.139
C_{70} 5 wt%	11.41	0.11	0.563	0.709	3.914	−3.851
MWCNT 1 wt %	11.20	0.18	3.433	4.293	18.778	−18.559
MWCNT 3 wt %	13.49	0.21	3.595	4.49	18.248	−18.658
MWCNT 5 wt %	14.94	0.50	3.664	4.574	18.412	−18.246

associated with the high filler concentration and the accumulation of surface particles on the sliding track. Tiny sized flake/chip particles deposit on the top of track surface which raises the friction coefficient. While testing the 5 wt% filler substrate under high load, once again the friction coefficient drops because of higher applied load and formation of smooth region (see Fig. 8d). At high sliding speed (1000 RPM) considered in the test, this higher load clears the deposits, which provides smooth region in the form of a protective layer over the substrate surface. It can be said that for all filler concentration of fullerene C_{70}, surface work mechanism in the form of smooth zone between the contact materials leads to decrease in friction coefficient at higher load.

At lower load limit, friction coefficient values of MWCNT (Fig. 7c) epoxy substrates is lower compared to fullerene C_{70} substrates. This is caused by the shearing of asperities and creation of smooth sliding zone with minimum contact area. A unique behavior of friction coefficient has been observed for 1 wt% MWCNT at 2N load. The measured value is ~0.07 which is similar to any machinery operating under full hydrodynamic lubrication condition [50]. In the particle detachment process the

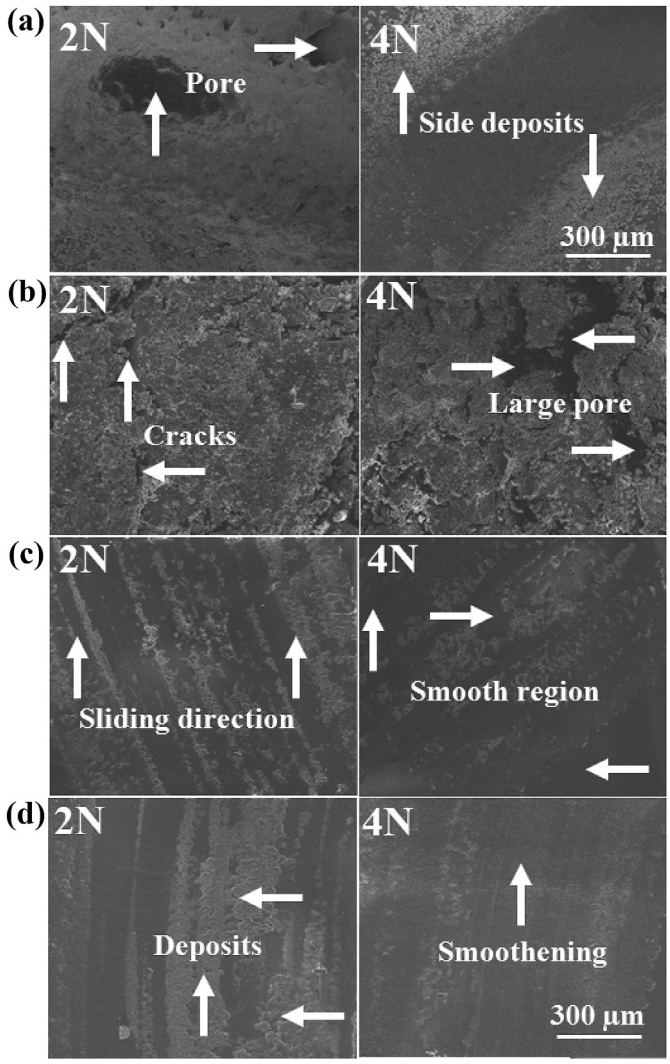


Fig. 8. SEM images of (a) pure epoxy (b) 1 wt% fullerene C_{70}, (c) 3 wt% fullerene C_{70} and (d) 5 wt% fullerene C_{70}.

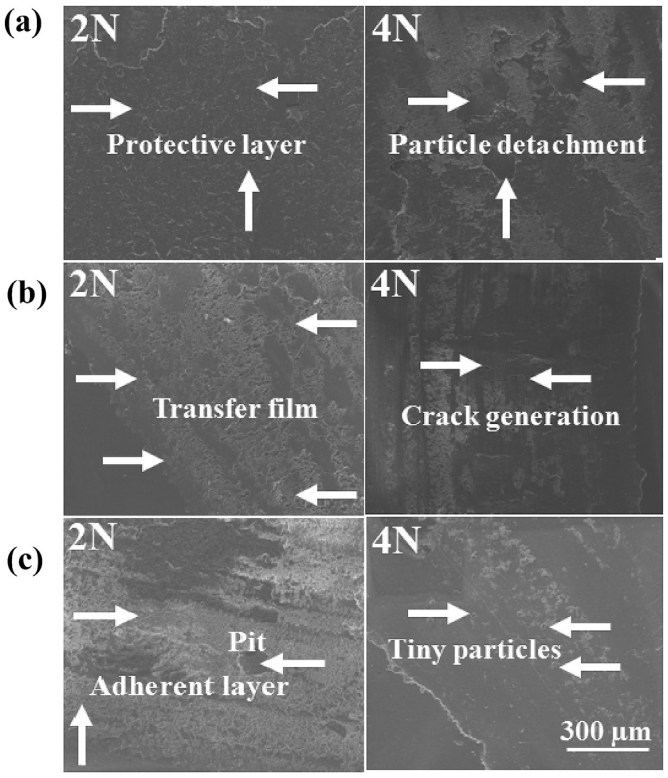


Fig. 9. SEM Images of infused (a) 1 wt% MWCNT, (b) 3 wt% MWCNT and (c) 5 wt% MWCNT.

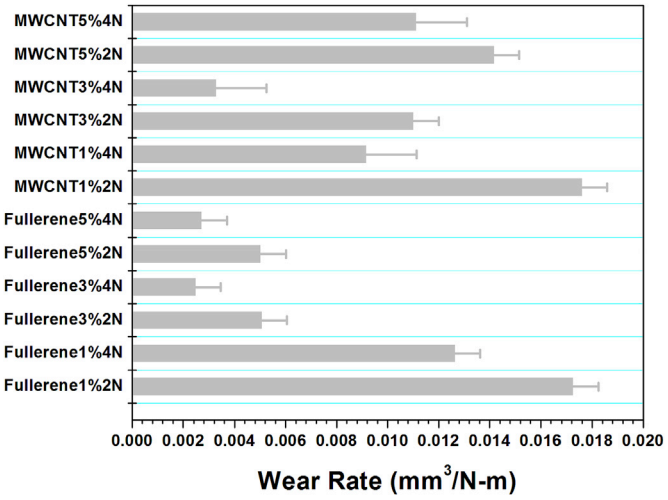


Fig. 10. Wear rate of tested filler epoxy substrates.

detached particles turn into a lubricious film layer over the substrate surface which decreases the friction coefficient (see Fig. 9a). Additionally, MWCNT has its own self lubricating property when mix within other composites [51]. At higher load of 4N more particles are detached which are filled between the two asperities and thus increase the surface contact area [52,53]. The increase in surface contact area leads to increase in the friction coefficient towards a higher value of ~0.17. In comparison to lower filler concentration, addition of 3 wt% and 5 wt% MWCNT into the epoxy has certainly increased the friction coefficient values. However, the wear rate of 3 wt% MWCNT at 4N load is minimum irrespective to the tiny crack generation on the surface (see Fig. 9b). Continuous flushing of particles from interspaces between the substrate surface and the ball fills the vacant pockets and thereby reduces the wear rate. At higher filler concentration of MWCNT, changes towards the starting and middle phase of the sliding contact have been observed due to inhomogeneous distribution of filler material. The influencing factor behind the high friction coefficient values is inhomogeneous dispersion of MWCNT in the epoxy matrix, which forms agglomerates (Fig. 9c) and produces high surface roughness. Most of the time is consumed by the steel counterpart material to make rough substrate surface smoother. However, if the heights of the peaks are higher, work done is not completely paid off and hence increases friction coefficient.

Wear mechanism of tested epoxy substrates can be directly correlated to its surface behavior. After each sliding test the microstructural images of pure and infused epoxy substrates were shown in Fig. 8a-d and Fig. 9a-c. Wear testing of pure epoxy substrate at normal load of 2N causes formation of pore because of sudden applied load, high speed of rotation and weak adhesion forces between the epoxy molecules, which create void space on the surface, see Fig. 8a [54]. Hence, the wear rate is high in the range of 10^{-2} mm^3/N-m due to severe asperity interaction and less available contact area. On the other hand, fullerene C_{70} 1 wt% has similar wear rate (Fig. 10) compared to pure epoxy substrates, which depends on surface crack formation and build up of several large diameter pore on the surface during sliding contact, see Fig. 8b. Pure epoxy and Fullerene C_{70} 1 wt% surface experience high shearing force, where the wear mechanism is associated to the surface flake formation which is accumulated in between the steel ball and the epoxy substrate [55]. This flake

formation and particle accumulation is the cause of two-body sliding wearing mechanism. A lower wear rate is achieved in the case of 3 wt% and 5 wt% fullerene C_{70} due to surface smoothening, see Fig. 8c and d. Sliding against higher weight concentration fills the bumps completely between the junctions and thus results in surface smoothening and high area contact. In general, the hardness of the steel balls is higher than all the epoxy substrates which cause epoxy substrate material to flow under the action of applied load. Lower concentration particle inclusion generates surface deposits, which are accumulated over track area. However, addition of high weight concentration fillers into the epoxy matrix decreases the influence of steel balls. In high filler concentrations the lower wear rate than 1 wt% fullerene C_{70} implies the effect of transfer film formation and build up of smooth region on the top of wear track [56]. The nature of the surface completely alters via transfer film formation due to chemical bonding between the outermost surfaces. After several attempts of sliding, the transfer film provides self protective layer between the sliding pair and decreases the wear rate.

In the case of 1 wt% MWCNT, the wear rate has not been lowered irrespective of having minimum friction coefficient. The wear rate is quite similar that for fullerene C_{70} 1 wt% (2N) because of unfilled valleys between the two asperity junctions. Surface contact area is enlarged by the filling of generated particles, however, these particles are easily flushed away from the surface and hence wear rate rises. The increment in wear rate at lower loads signifies the instability of protective film over the surface. These films are unstable and get detached (see Fig. 9a) from the substrate surface as soon as sliding occurs. On the other hand, as the filler concentration is increased to 3% the wear rate is significantly reduced at 4N load due to stable film which is necessary to fill up the valleys, see Fig. 9b. As seen from Fig. 9c further increase in filler concentration to 5 wt% gives adhered particles at the top of the substrate surface. The rise in wear rate at this concentration is caused by the filler accumulation at the contact zone. A non-protective dense layer has been formed by the action of sliding which increases wear rate.

Hence, from wear point of view, two general conclusions can be drawn from the results presented. First, wear rate increases due to scratching or peeling of particles (epoxy/epoxy-filler) from the substrate surface soon after sliding occurs. If the generated wear particles are in sliding motion, they acquire large contact area to move across the substrate surface. At the same time, detachment of more wear particles will be triggered from the nearby substrate surface, which ultimately increase overall wear rate. The second conclusion is that, if the nature of the generated particles is rolling instead of sliding then the contact area will be relatively much lower. Rolling particles move across the surface with less contact and provide minimum detachment, which gives rise to less wear rate compared to the sliding situation. Therefore, sliding and rolling turn out to be a dominant factor which is discussed later in discussion on wear mechanism.

Fig. 11 shows the ball scar and corresponding wear track after each tribological test. Three different categories of track deposition can be identified as high, medium and low dark patches. During sliding test a thick layer has been formed on the substrate surface by the action of continuous rubbing. This thick layer grows after each sliding cycle on the top of fullerene C_{70} and MWCNT substrate surfaces. High dark patches signify towards increased rate of wear and friction coefficient, as in case of epoxy fullerene C_{70} (1 wt%) and epoxy MWCNT (5 wt%). Deposits of medium dark patches over epoxy fullerene C_{70} (5 wt%) and epoxy MWCNT (3 wt%) substrates leads optimum friction coefficient and wear rate. Deposits of low dark patches over epoxy fullerene C_{70} 3 wt% gives low friction values with minimum wear rate. In the case of epoxy 1 wt% MWCNT substrate, irrespective of ultra low friction coefficient the wear rate is increased due to continuous flushing of 1 wt% MWCNT particles from the valleys. Ball images of epoxy fullerene C_{70} show some inclusions which are transferred from the substrate side, see Fig. 11a. These inclusions favor to reduce friction coefficient and wear rate. However, large inclusions at higher load of MWCNT triggered the increase of wear and friction coefficient, see Fig. 11b. In the case of MWCNT (1 wt%, 2N load), steel ball did not wear at all. Nevertheless, sliding past 10^4 numbers of cycles increases wear rate due to non availability of particles which are necessary to fill each bumps and provide smooth riding to the ball. The dark layer on the epoxy wear tracks results in the formation of carbon patches during the sliding test [57]. These carbon patches are the significant contributor towards lowering the COF value. The surface plowing by steel balls are abrasive in nature which generates grit particles. The size of the grit particles ranges from few microns to several microns in length stuck towards either ball side or substrate side. Sometimes, depending on the true surface behavior and the test conditions, the measured tribological values are increased or decreased due to sticking of these grit particles.

Based on the wear data results and SEM micrographs, the sliding wear mechanism of epoxy/fullerene C_{70} and epoxy/MWCNT is illustrated in Fig. 12. The major proportion is abrasive wear as a result of hard particle detachment from the worn surface. These fragments are in either sliding or rolling contact (Fig. 12a and b) between the steel counterpart and the epoxy substrate. The sliding and rolling fragments are known as two-body and three-body abrasive wear, respectively. The three-body abrasive wear is a less dominant phenomenon than the two-body, because loose particles are free to roll across the surface, where rolling contact area is less than that of sliding contact area [57]. Friction coefficient and wear rate generally depends on the true contact nature of these generated particles. The second foremost influential mechanism is transfer film formation (Fig. 12c), which reduces wear rate of epoxy substrates. This transfer film has built up after several attempt of sliding cycles and formed between the contact pair to resist any further material loss. Thickness of the transfer film increases with number of sliding cycles, but diminishes from the surface as soon as the adhesive force between the transfer film and the steel counterface material is weaken than the force between transfer film and the epoxy substrate surface [58]. It is found that COF and wear rate are reduced by the addition of fullerene C_{70} and MWCNT into the epoxy matrix, which lowered the steel ball penetration over the surface by forming a transfer film. However, more detachment from the surface is a result of few weak zones formation during initial processing of epoxy/fullerene C_{70} and epoxy/MWCNT substrates. Accumulation in the form of surface deposits (Fig. 12d) reduces the capability of transfer film and provides plowing action, which further increases friction coefficient and wear rate.

In this study, tribological mechanism and utilization of epoxy/fullerene C_{70}/MWCNT have been proposed on the basis of experimental observations. Based on the present research work it can be said that nominal particle concentration improves the surface functionalization in terms of friction and wear with structural integrity. Epoxy based composites are proven to be compatible with carbon materials for infusing with these materials. Other researchers [36,37] have found high friction coefficient of tested fullerene under silicon/steel contact mode, which ranges between 0.4 and 1.0, or sometimes even higher. In our observation, the maximum friction coefficient values of epoxy/fullerene C_{70}/MWCNT were only up to 0.29, which makes these infused epoxy composites suitable for automotive components.

4. Conclusions

The present work investigates chemical, physical, thermal and tribological properties of carbon based filler. Fullerene C_{70} and multi-walled carbon nanotubes have proven to be excellent performers for infusion into the epoxy matrix for improving the tribological behavior. The following conclusions are drawn from the present study.

1. The phase change in prepared samples is a characteristic of interfacial interaction between filler substitute and epoxy itself while curing from room temperature to 100 °C. High wave-number of tested samples reveals carboxyl and hydroxyl functional group at particular intensities. XPS bonding state represents major proportion of carbon-carbon and carbon-oxygen.

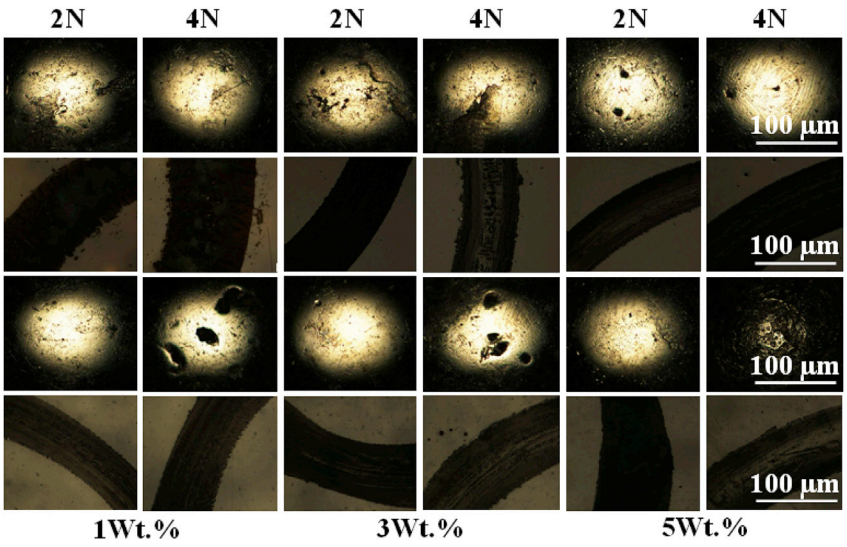


Fig. 11. Optical microscope images of ball scar and track wear after performing the tribological tests on (a) epoxy fullerene C_{70} and (b) MWCNT at 2N and 4N load.

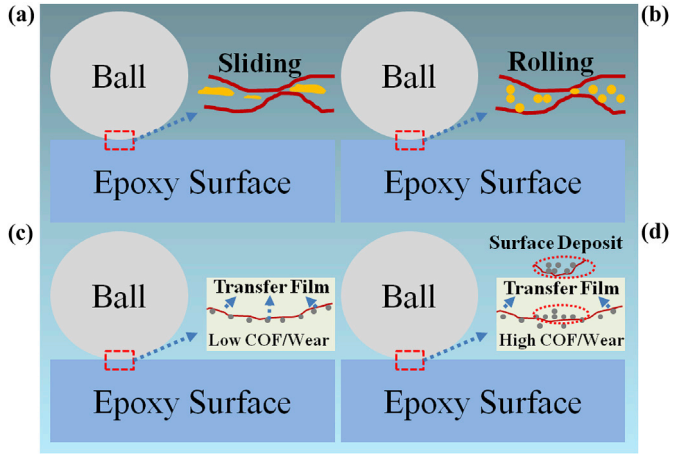


Fig. 12. Major wear mechanism of (a) abrasive - two body contact, (b) abrasive - three body contact, (c) transfer film formation and (d) surface deposit.

2. High glass transition temperature of the embedded carbon materials results from high temperature curing process and intrinsic bonding between the epoxy-filler molecules at the materials structure.
3. Surface wetting behavior is most favorable in the case of high filler concentration. The measured contact angle values of fullerene C_{70} and MWCNT is below 90°. In the presence of water and oil medium, the optimum values of 5 wt% fullerene C_{70} and 5 wt% MWCNT are 61°, 10.9° and 56.9°, 11.7°, respectively. The highest achieved surface energy value for 5 wt% fullerene C_{70} and 5 wt% MWCNT is 47.23 and 44.94 mJ/m^2, respectively.
4. Increase in particle concentration increases the hardness (HV) of the substrate. The hardness of 5 wt% fullerene C_{70} and MWCNT is 11.41, 14.94, respectively. Also, surface roughness (Ra) of the samples is increased from 0.465 to 0.563 and 3.433 to 3.664 for 1 to 5 wt% increase in fullerene C_{70}, MWCNT, respectively.
5. Friction coefficient of infused fullerene C_{70} and MWCNT substrates were in the range of 0.17–0.29, 0.07–0.27, respectively. The wear rate is in the range of 10^{-3} -10^{-2} mm^3/N-m. Friction coefficient of 1 wt% MWCNT at 2N load is ~0.07, which is a key improvement in surface resistance against dry sliding contact.

Acknowledgements

This work is supported by the Science & Engineering Research Board (SERB), New Delhi, India, Grant No. PDF/2016/001408.

References

[1] Gao Q, Adarme JL, Paul BK, Haapala KR. An economic and environmental assessment model for microchannel device manufacturing: part 1 – Methodology. J Clean Prod 2016;120:135–45.
[2] Wan S, Tieu AK, Xia Y, Zhu H, Tran BH, Cui S. An overview of inorganic polymer as potential lubricant additive for high temperature tribology. Tribol Int 2016;102:620–35.
[3] Chowdhury MA, Helali M. The effect of relative humidity and roughness on the friction coefficient under horizontal vibration. Open Mech Eng J 2008;2:128–35.
[4] Kanchanomai C, Noraphaiphipaksa N, Mutoh Y. Wear characteristic of epoxy resin filled with crushed-silica particles. Composites: Part B 2011;42:1446–52.
[5] Zhai W, Srikanth N, Kong LB, Zhou K. Carbon nanomaterials in tribology. Carbon 2017;119:150–71.
[6] Tagawa M, Yokota K, Kishida K, Okamoto A, Minton TK. Energy dependence of hyperthermal oxygen atom erosion of a fluorocarbon polymer: relevance to space environmental effects. ACS Appl Mater Interfaces 2010;2(7):1866–71.
[7] Krella AK. Degradation of AlMg2 aluminium alloy caused by cavitation — an effect of cavitation intensity. Mater Char 2017;130:219–29.
[8] Lee MW, Sett S, Yoon SS, Yarin AL. Fatigue of self-healing nanofiber-based composites: static test and subcritical crack propagation. ACS Appl Mater Interfaces 2016;8(28):18462–70.
[9] Oláh N, Fogarassy Z, Sulyok A, Szívós J, Csanádi T, Balázsi K. Ceramic TiC/a:C protective nanocomposite coatings: structure and composition versus mechanical properties and tribology. Ceram Int 2016;42:12215–20.
[10] Horng JH. Studies of tribological behavior and separation between surfaces at initial boundary lubrication. Wear 1998;216:8–14.
[11] Davis B, Schueller JK, Huang Y. Study of ionic liquid as effective additive for minimum quantity lubrication during titanium machining. Manuf Lett 2015;5:1–6.
[12] Candelario VM, Moreno R, Guiberteau F, Ortiz AL. Enhancing the sliding-wear resistance of SiC nanostructured ceramics by adding carbon nanotubes. J Eur Ceram Soc 2016;36:3083–9.
[13] Moghadam AD, Omrani E, Menezes PL, Rohatgi PK. Mechanical and tribological properties of self-lubricating metal matrix nanocomposites reinforced by carbon nanotubes (CNTs) and graphene – a review. Compos B Eng 2015;77:402–20.
[14] Zhang L, Pu J, Wang L, Xue Q. Frictional dependence of graphene and carbon nanotube in diamond-like carbon/ionic liquids hybrid films in vacuum. Carbon 2014;80:734–45.
[15] Santhosh V, Voggu R, Chaturbedy P, Ganapathy R, Rao CNR. Mechanical properties of C60 thin films at the air-water interface. Carbon 2016;96:1–5.
[16] Zhang SW. State-of-the-art of polymer tribology. Tribol Int 1998;31:49–60. 1998.
[17] Bourgeat-Lami E, Lansalot M. Organic/inorganic composite latexes, the marriage of emulsion polymerization and inorganic chemistry. Adv Polym Sci 2010;233:53–123.
[18] Gudarzi MM, Sharif F. Molecular level dispersion of graphene in polymer matrices using colloidal polymer and graphene. J Colloid Interface Sci 2012;366(1):44–50.
[19] Bourgeat-Lami E, Faucheu J, Noëlab A. Latex routes to graphene-based nanocomposites. Polym Chem 2015;6:5323–57.
[20] Kobayashi M, Matsugi T, Saito J, Imuta JI, Kashiwab N, Takahara A. Direct modification of polyolefin films by surface-initiated polymerization of a phosphobetaine monomer. Polym Chem 2013;4:731–9.

[21] McElwain SE, Blanchet TA, Schadler LS, Sawyer WG. Effect of particle size on the wear resistance of alumina-filled PTFE micro- and nanocomposites. Tribol Trans 2008;51:247–53.
[22] Chen BB, Wang JZ, Yan FY. Synergism of carbon fiber and polyimide in polytetrafluoroethylene-based composites: friction and wear behavior under sea water lubrication. Mater Des 2012;36:366–71.
[23] McElwain SE, Blanchet TA, Schadler LS, Sawyer WG. Effect of particle size on the wear resistance of alumina-filled PTFE micro- and nanocomposites. Tribol Trans 2008;51:247–53.
[24] Wypych G. Handbook of fillers4. Toronto, Ontario, Canada: ChemTec Publishing; 2016. p. 1–12.
[25] Jin FL, Li X, Park SJ. Synthesis and application of epoxy resins: a review. J Ind Eng Chem 2015;29:1–11.
[26] Balakrishnan S, Start PR, Raghavan D, Hudson SD. The influence of clay and elastomer concentration on the morphology and fracture energy of preformed acrylic rubber dispersed clay filled epoxy nanocomposites. Polymer 2005;46:11255–62.
[27] Singh V, Joung D, Zhai L, Das S, Khondaker SI, Seal S. Graphene based materials: past, present and future. Prog Mater Sci 2011;56:1178–271.
[28] Brostowa W, Chonkaewa W, Menarda KP, Scharf TW. Modification of an epoxy resin with a fluoroepoxy oligomer for improved mechanical and tribological properties. Mater Sci Eng 2009;507:241–51.
[29] Zhang G, Sebastian R, Burkhart T, Friedrich K. Role of mono dispersed nanoparticles on the tribological behavior of conventional epoxy composites filled with carbon fibers and graphite lubricants. Wear 2012;292–293:176–87.
[30] Bahadur S, Sunkara C. Effect of transfer film structure, composition and bonding on the tribological behaviour of polyphenylene sulfide filled with nano particles of TiO_2, ZnO, CuO and SiC. Wear 2005;258:1411–21.
[31] Shen XJ, Pei XQ, Fu SY, Friedrich K. Significantly modified tribological performance of epoxy nanocomposites at very low graphene oxide content. Polymer 2013;54:1234–42.
[32] Zhang J, Chang L, Deng S, Ye L, Zhang Z. Some insights into effects of nanoparticles on sliding wear performance ofepoxy nanocomposites. Wear 2013;304:138–43.
[33] Yu S, Hua H, Ma J, Yin J. Tribological properties of epoxy/rubber nanocomposites. Tribol Int 2008;41:1205–11.
[34] Melk L, Rovira JJR, Antti ML, Anglada M. Coefficient of friction and wear resistance of zirconia–MWCNTs composites. Ceram Int 2015;41:459–68.
[35] Al-Kawaz A, Rubin A, Badi N, Blanck C, Jacomine L, Janowska I, Pham-Huu C, Gauthier C. Tribological and mechanical investigation of acrylic-based nanocomposite coatings reinforced with PMMA-grafted-MWCNT. Mater Chem Phys 2016;175:206–14.
[36] Zhao W, Tang J, Puri A, Sweany RL, Li Y, Chen L. Tribological properties of fullerenes C_{60} and C_{70} microparticles. J Mater Res 1996;11(11):2749–56.
[37] Zhao W, Tang J, Li Y, Chen L. High friction coefficient of fullerene C_{70} film. Wear 1996;198:165–8.
[38] Boeva ZA, Milakin KA, Pesonen M, Ozerin AN, Sergeyev VG, Lindfors T. Dispersible composites of exfoliated graphite and polyaniline with improved electrochemical behaviour for solid-state chemical sensor applications. RSC Adv 2014;4:46340–50.
[39] Kumar S, Asokan K, Singh RK, Chatterjee S, Kanjilal D, Ghosh AK. RSC Adv 2014;4:62123–31.
[40] Chase B, Herron N, Holler E. Vibrational spectroscopy of C_{60} and C_{70} temperature-dependent studies. J Phys Chem 1992;96:4262–6.
[41] Zardini HZ, Davarpanah M, Shanbedi M, Amiri A, Maghrebi M, Ebrahimi L. Microbial toxicity of ethanolamines-multiwalled carbon nanotubes, 102; 2014. p. 1774–81. 6.
[42] Jensen K, Mickelson W, Kis A, Zettl A. Buckling and kinking force measurements on individual multiwalled carbon nanotubes. Phys Rev B 2007;76(19). pp. 195436–5.
[43] Rojasa JV, Toro-Gonzaleza M, Molina-Higgins MC, Castano CE. Facile radiolytic synthesis of ruthenium nanoparticles on grapheneoxide and carbon nanotubes. Mater Sci Eng B 2016;205:28–35.
[44] Kwok DY, Lam CNC, Li A, Zhu K, Wu R, Neumann AW. Low-rate dynamic contact angles on polystyrene and the determination of solid surface tensions, 38; 1998. p. 1675–84.
[45] Neumann AW, Good RJ, Hope CJ, Sejpal M. An equation-of-state approach to determine surface tensions of low-energy solids from contact angles. J Colloid Interface Sci 1974;49:291–304.
[46] Pawlaka Z, Urbaniak W, Oloyede A. The relationship between friction and wettability in aqueous environment. Wear 2011;271:1745–9.
[47] Borruto A, Crivellone G, Maran F. Influence of surface wettability on friction and wear tests. Wear 1998;222:57–65.
[48] Pawlak, Petelska Z, Urbaniak AD, Yusuf W, Oloyede KQ. A relationship between wettability and lubrication characteristics of the surfaces of contacting phospholipid-based membranes. Cell Biochem Biophys 2013;65:335–45.
[49] Ghorbal A, Bistac S, Schmitt M. Friction and nanowear of polystyrene against hydrophobic and hydrophilic substrates. J Polym Sci B Polym Phys 2006;44:2449–54.
[50] Zhang X, Kanapathipillai S, Wu T, Peng Z. Frictional behaviour and friction mechanisms of rolling-sliding contact in mixed EHL. Tribol Int 2017;114:201–7.
[51] Gong G. Natural polymers: nanocomposites. RSC 2012:150–84.
[52] Mo YF, Turner KT, Szlufarska I. Friction laws at the nanoscale. Nature 2009;457:1116–9.
[53] Karuppiah KSK, Bruck AL, Sundararajan S. Evaluation of friction behavior and its contact-area dependence at the micro- and nano-scales. Tribol Lett 2009;36:259–67.
[54] Hou PY, Priimak K. Interfacial segregation, pore formation, and scale adhesion on NiAl alloys. Oxid Metals 2005;63(1):113–30.
[55] Goyal RK, Yadav M. Study on wear and friction behavior of graphite flake-filled PTFE composites. J Appl Polym Sci 2013;127(4):3186–91.
[56] Ye J, Burris DL, Xie T. A review of transfer films and their role in ultra-low-wear sliding of polymers. Lubricants 2016;4:1–15.
[57] Gates JD. Two-body and three-body abrasion: a critical discussion. Wear 1998;214(1):139–46.
[58] Sukumaran J, Pauw JD, Neis PD, Tóth LF, Baets PD. Revisiting polymer tribology for heavy duty application. Wear 2017;376-377:1321–32.